



From Fish Scale Gelatin to Tyrosinase Inhibitor: A Novel Peptides Screening Approach Application

Zi-Zi Hu¹, Xiao-Mei Sha^{1*}, Lu Zhang¹, Min-Jun Zha¹ and Zong-Cai Tu^{1,2*}

¹ National R&D Center for Freshwater Fish Processing, College of Chemistry and Chemical Engineering & College of Life Science, Jiangxi Normal University, Nanchang, China, ² State Key Laboratory of Food Science and Technology, Nanchang University, Nanchang, China

OPEN ACCESS

Edited by:

Qiang Xia,
Ningbo University, China

Reviewed by:

Hongshun Yang,
National University of
Singapore, Singapore
Liqiang Zou,
Nanchang University, China

*Correspondence:

Xiao-Mei Sha
shaxiaomei1987@sina.com
Zong-Cai Tu
004756@jxnu.edu.cn

Specialty section:

This article was submitted to
Food Chemistry,
a section of the journal
Frontiers in Nutrition

Received: 12 January 2022

Accepted: 07 February 2022

Published: 18 March 2022

Citation:

Hu Z-Z, Sha X-M, Zhang L, Zha M-J
and Tu Z-C (2022) From Fish Scale
Gelatin to Tyrosinase Inhibitor: A Novel
Peptides Screening Approach
Application. *Front. Nutr.* 9:853442.
doi: 10.3389/fnut.2022.853442

Bioaffinity ultrafiltration combined with LC-Orbitrap-MS/MS was applied for the first time to achieve rapid screening and identification of tyrosinase inhibitory peptides (TYIPs) from grass carp scale gelatin hydrolysates. The binding mode of TYIPs with tyrosinase was investigated by molecular docking technology. The whitening effect of TYIPs was further studied by evaluating the tyrosinase activity and melanin content in mouse B16F10 cells. Four new TYIPs were screened from hydrolysates, among which DLGFLARGF showed the strongest tyrosinase inhibition with an IC₅₀ value of 3.09 mM. Molecular docking showed that hydrogen bonds were the main driving force in the interaction between the peptide DLGFLARGF and tyrosinase. The addition of DLGFLARGF significantly inhibited the tyrosinase activity and melanin production of B16F10 melanoma cells. These results suggest that DLGFLARGF is a promising skin whitening agent for the treatment of potential pigment-related diseases.

Keywords: grass carp scale gelatin, tyrosinase inhibitory peptides, bioaffinity ultrafiltration, LC-Orbitrap-MS/MS, whitening

INTRODUCTION

Gelatin has a rich sources and is widely used in the food and medicine industries (1–5). The hydrolysis product of gelatin is collagen peptide, which is a mixture of peptides. After separation and purification, specific bioactive peptides could be obtained that have a wide range of significant functional activities. At present, the functional activities of collagen peptides such as antioxidant activity (6), angiotensin-converting enzyme inhibition activity (7), anti-tumor activity (8), and antibacterial activity (9) have been studied. Recent studies have shown that many active peptides contain some hydrophobic amino acids, uncharged polar amino acids, aromatic amino acids, etc., which have the ability to inhibit the production of melanin (10, 11).

The production of melanin is regulated by enzymes such as tyrosinase, tyrosinase-binding protein-1 (dopa pigment isomerase), and tyrosinase-binding protein-2 (melanin precursor oxidase) (12). Tyrosinase (EC1.14.18.1) is a multifunctional enzyme with three histidine (His) residues and two Cu ions in the active center, which is widely found in fungi, plants and animals. Tyrosinase oxidizes tyrosine to produce dopamine and then continues to oxidize dopamine to produce dopamine quinone. Dopamine quinone is a very active molecule that can generate a polymer complex or brownish pigment when it reacts with amino acids or proteins, finally producing melanin (13). Substances with tyrosinase inhibition activity are commonly found in whitening foods. At present, tyrosinase inhibitors widely used in foods have been reported, including arbutin,

kojic acid, oxidative resveratrol, etc. (14). However, studies have shown that these substances show limiting effects and certain side effects, including the lack of good permeability, high toxicity and poor stability (15). Scientists have recently become interested in the tyrosinase inhibitory activity of extracts from natural sources, due to the benefits of mild functional activity, simple absorption, and excellent skin compatibility (16–18). Active polypeptide is composed of 2–20 amino acids, which has the above advantages that could provide the possibility for its application in foods (19).

The conventional procedures for screening active peptides from complex protein hydrolysates include the preparation of hydrolysates, bioassay-guided separation, purification and peptide sequence identification. In general, traditional methods require multi-step extraction and separation with organic solvents, resulting in low efficiency, serious environmental pollution, time-consuming and laborious (20, 21). The combination of bioaffinity ultrafiltration and liquid chromatography-mass spectrometry based on the interaction between small molecule ligands and enzyme active sites is an effective approach for a powerful approach for identifying biologically active compounds from complex mixtures (22). It has been widely used to screen and identify a variety of biologically active compounds from natural extracts and traditional Chinese medicine (23). Qin et al. (24) established a bioaffinity ultrafiltration-high performance liquid chromatography-electrospray ionization-time of flight-mass spectrometry (BAUF-HPLC-ESI-TOF/MS) method to identify potential new bioactive substances. This method has been demonstrated to be a quick way to obtain high-purity, high-activity bioactive substances. However, there is no report about screening tyrosinase inhibitor peptides by this method.

In this paper, a rapid screening and identification method for the tyrosinase inhibitory peptides (TYIPs) in the hydrolysis of fish scale (by-products during freshwater fish production) gelatin was established for the first time based on ultrafiltration and Nano-LC-Orbitrap-MS/MS. Then, molecular docking was used to determine the interaction of the identified peptide with tyrosinase in order to investigate the biological activity and mechanism. Finally, the effect of peptides on B16F10's ability to produce melanin was further studied.

MATERIALS AND METHODS

Materials

Grass carp scale gelatin was obtained from the laboratory. Alcalase ($\geq 200,000$ units/g) was purchased from Solarbio Chemical Co. (Shanghai, China). Mushroom tyrosinase (6,680 U/mg) and 3,4-dihydroxyphenylalanine (L-DOPA) were purchased from Sigma-Aldrich (St. Louis, MO, USA). The murine melanoma B16F10 cells (CL0039) were acquired from Fenghui Biological Technology Co., Ltd. (Hunan, China). All the other reagents were analytical grade.

Preparation of TYIPs From Fish Scale Gelatin

The grass carp scale gelatin was prepared according to the method of Sha et al. (25). According to previous experiments,

the optimal enzymatic hydrolysis conditions for preparing TYIPs were: substrate concentration of 125 mg/ml, alcalase dosage of 1%, pH 9.0, enzymatic hydrolysis temperature of 60°C, and enzymatic hydrolysis time of 2 h.

Analysis of the Tyrosinase Inhibitory Activity

The determination of the tyrosinase inhibitory activity was made according to Uysal et al. (26). Sample solutions (50 μ l) with the appropriate concentration were reacted with 50 μ l of 200 mM pH 6.8 phosphate buffer saline (PBS) solution and 50 μ l of tyrosinase at room temperature for 15 mins. Then, 50 μ l of 2.5 mM L-DOPA was added, and allowed to react at 30°C for 10 min. The absorbance (A_s) at 475 nm was finally measured with a microplate reader (Synergy H1, BioTek Co., Ltd., USA). Taking the reaction system without enzyme and sample as a blank. Kojic acid (2 mg/ml) used as the positive control, and the rate of tyrosinase inhibition could be calculated using the following equation:

$$\text{Tyrosinase inhibition rate/\%} = \frac{(A_c - A_b) - (A_s - A_b)}{(A_c - A_b)} \times 100\% \quad (1)$$

where, A_s is the absorbance of the sample after reaction; A_c is the absorbance of the reaction system with distilled water instead of the sample; A_b is the absorbance of the reaction system with distilled water instead of tyrosinase.

Analysis of the Amino Acid Composition

The amino acid composition was determined based on the report of Chen et al. (27) with appropriate modifications. The samples were hydrolyzed with 6 M HCl at 110°C for 24 h prior to composition analysis with a High-Speed Amino Acid Analyzer Model L-8900 (Hitachi Co., Japan).

Analysis of Molecular Weight Distribution

The molecular weight (MW) distribution was determined using an Agilent 1260 Infinity HPLC system (Agilent Technologies, Inc., Santa Clara, CA, USA) equipped with a waters XBridge Protein BEH 125Å SEC (3.5 μ m, 7.8 \times 300 mm) (28). Hydrolysates were eluted with water (0.1% FA) and acetonitrile (60:40, V/V) at a flow rate of 0.4 ml/min. The injection volume was 10 μ l. The detection wavelength was 220 nm (28). The MW of peptides was calculated based on the calibration curve constructed with cytochrome C (12,384 Da), aprotinin (6,511.51 Da), bacitracin (1,422.69 Da), L-oxidized glutathione (612.63 Da) and hydroxyproline (131.13 Da).

Rapid Screening of TYIPs Bioaffinity Ultrafiltration

The screening method was slightly modified based on the previous report (22). The inhibitory activity of tyrosinase was evaluated at 1–6 mg/ml to obtain the best binding concentration.

4 ml of hydrolysis product (5 mg/ml) and 2 ml of mushroom tyrosinase (10 U/ml) were incubated for 1 h at 37°C. Inactivated mushroom tyrosinase (heated in a

boiling water bath for 10 mins) was also prepared as a blank group. The detailed method is shown in **Figure 2A**. Filtrates, including peptides binding active tyrosinase (PAT) and peptides binding inactive tyrosinase (PIT), were collected and freeze-dried for tyrosinase inhibition evaluation and peptide identification.

Peptide Identification

The amino acid sequence of the components obtained in 2.6.1 was determined by Nano-LC-ESI-Q-Orbitrap-MS/MS. Peptides were separated on an AcclaimR PepMap RSLC (50 μ m \times 150 mm, C18, 2 μ m, 100 Å) column at a flow rate of 220 nl/min. Mobile phase A and B was consisted of 0.1% formic acid aqueous solution and 0.1% acetonitrile solution, respectively. Gradient elution conditions were as follows: 0–2 min, 4–12% B; 2–25 min, 12–22% B; 25–32 min, 22–32% B; 32–37 min, 32–75% B; 37–40 min, 75% B (isoelection). The positive ion scanning mode was adopted, and the mass spectrometry data were collected using Xcalibur 2.2 SP1 software, with a mass range of 250–1,250 m/z and a resolution of 70,000. The top 20 peptides were selected for fragmentation according to the signal strength of the first mass spectrometry, and the fragmentation mode was HCD with an energy of 27%. The parent ion map was analyzed by Xcalibur software and De Novo was sequenced using PEAKS Studio 7.0 software to obtain the amino acid sequence of peptides. The peptides identified in this paper met the requirements of false discovery rate (FDR) \leq 5% and average local confidence score (ALC) \geq 95%.

Molecular Docking and Peptides Synthesis

The X-ray crystal structure of *Agaricus bisporus* tyrosinase (2Y9W) was downloaded from the Protein Data Bank (<https://www.rcsb.org/structure/2Y9W>) (29), and three-dimensional (3D) structure of TYIPs segment were obtained by ChemBio 3D Ultra 14.0. Based on the 3D crystal structure of tyrosinase, the computer-aided technology was used to analyze the action mode and site of peptide segment with tyrosinase, and to clarify the action mechanism. The specific docking process was as follows: first, the AutoDock tool is used to remove water molecules from tyrosinase and add Gasteiger charges and hydrogen atoms to tyrosinase molecules. Then, the AutoDock tool was used again to dock ligand small molecules (peptides) with tyrosinase. The docking process and calculation were carried out according to default parameters. The coordinates of the docking center of the peptide with tyrosinase were (64, 70, 116). Results were obtained based on the lowest free energy.

Cell Culture

B16F10 cells were kept in Dulbecco's modified eagle medium supplemented with 10% heat-inactivated fetal bovine serum, and cells were cultured at 37°C in an atmosphere with 5% CO₂. These cells were then used for cell viability, tyrosinase inhibition and melanin content determination.

Determination of the Cell Viabilities of B16F10 Melanoma Cells

The previously described cell counting kit-8 (CCK-8) assay was used to assess cell viability (30). The cells were incubated in a 96-well plate with 5×10^4 cells per well in a 5% humid CO₂ atmosphere at 37°C for 24 h. DLGFLARGF was added to the cells at concentrations of 0, 0.1, 0.2, 0.4, 0.8 and 1.6 mg/ml, while 0.75 mg/ml of kojic acid was used as a positive control. The cells were re-incubated for 24 h under the same conditions. The cells were then treated with the CCK-8 reagent and incubated at 37°C for 1 h. Cell viability is calculated by reading the absorbance value at 450 nm. The calculation formula is shown below.

$$\text{Cell viability}/\% = \frac{(A_s - A_b)}{(A_c - A_b)} \times 100\% \quad (2)$$

where, A_s is the absorbance of experimental wells (medium containing cells, CCK-8, sample to be tested); A_c is the absorbance of control well (medium containing cells, CCK-8, no sample to be tested); A_b is the absorbance of blank wells (medium without cells and samples to be tested, CCK-8).

Determination of Tyrosinase Activity in B16F10

The tyrosinase inhibition was determined according to the method of Ullah et al. (31). B16F10 cells were seeded into 96-well plates at a rate of 5×10^4 cells per well and incubated at 37°C in a humid atmosphere of 5% CO₂ for 24 h. The cells were then treated with kojic acid (0.75 mg/ml) and DLGFLARGF (0, 0.1, 0.2, 0.4, 0.8 and 1.6 mg/ml), and re-incubated for 24 h under the same conditions. The cells were then washed with PBS buffer, lysed with lysate buffer [100 μ l containing 50 mM PBS, 0.1 mM phenylmethanesulfonyl fluoride (5 μ l) and Triton X-100 (5 μ l)], and frozen at -80°C for 30 min. The cell lysate was then centrifuged at 12,000 rpm at 4°C for 30 min and transferred to a 96-well plate with a total volume of 100 μ l (80 μ l lysate supernatant and 20 μ l 10 mM L-DOPA) and incubated for 30 min at 37°C. The absorbance was measured at 450 nm using an enzyme-linked immunosorbent assay (ELISA) reader.

Determination of Melanin Content in B16F10

After cultivated according to the instructions above, the cells were digested with 0.25% trypsin when reached to 80–90% confluence to make a single cell suspension. Fresh culture medium was used to adjust the cell concentration to 1×10^6 cells/ml, 2 ml of which was inoculated in a 6-well culture plate for incubation overnight. When the cells adhered, the supernatant was discarded and the cells were rinsed with PBS once. 2 ml fresh culture medium was added again for incubation under CO₂ for 48 h. The supernatant was discarded after the incubation, and the adhered cells were rinsed with PBS and then dispersed with trypsin. The dispersed cells were collected and centrifuged at 1,500 r/min for 10 min. The precipitation was added with

1 ml NaOH (1 mol/L) containing 10% dimethyl sulfoxide for 1 h water bath at 80°C before being transferred to a 96-well culture plate. Measured the optical density value of each well

at 405 nm with a microplate reader, and calculated the melanin content (32).

$$\text{Melanin content}/\% = \frac{(A_s - A_b)}{(A_c - A_b)} \times 100\% \quad (3)$$

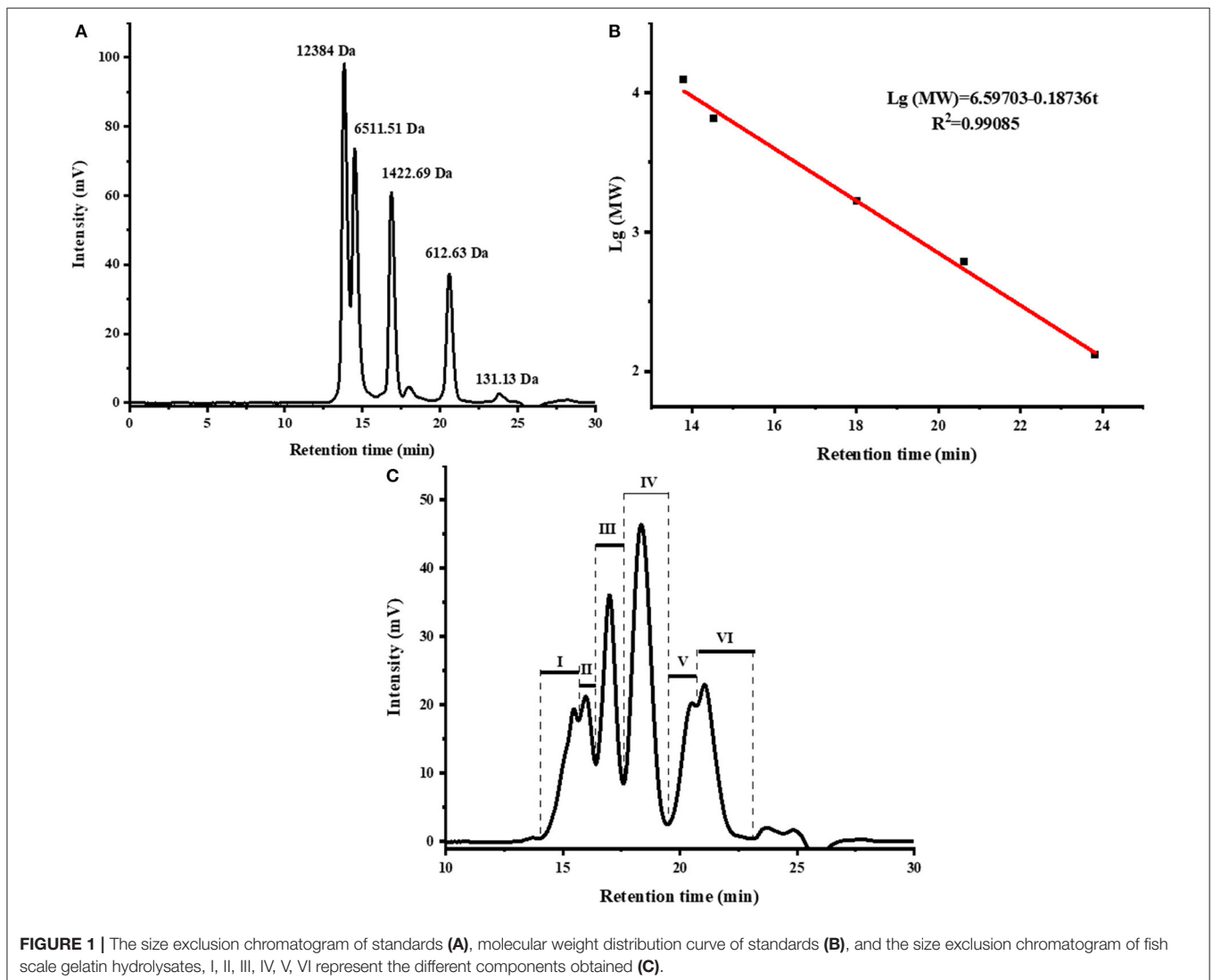
TABLE 1 | Amino acid composition of fish scale gelatin hydrolysate.

Amino acid	Content (g per 100 g)	Amino acid	Content (g per 100 g)
Asp	4.58 ± 0.16	Ile [*]	1.03 ± 0.02
Thr	2.00 ± 0.05	Leu [*]	2.60 ± 0.08
Ser	2.49 ± 0.05	Tyr	0.41 ± 0.05
Glu	7.82 ± 0.16	Phe [*]	1.53 ± 0.03
Gly	16.71 ± 0.03	Lys	2.83 ± 0.03
Ala [*]	5.58 ± 0.04	His	0.26 ± 0.01
Cys	0.05 ± 0.01	Arg	6.74 ± 0.01
Val [*]	1.83 ± 0.04	Pro [*]	9.43 ± 0.07
Met [*]	1.24 ± 0.07		

^{*}Hydrophobic amino acid.

TABLE 2 | Molecular weight distribution of fish scale gelatin hydrolysate.

Component	Molecular weight range (Da)	Retention time (min)	Relative content (%)	Peak molecular weight (Da)
I	9,217–4,642	14.05–15.64	9.75	4,974
II	4,642–3,358	15.64–16.39	8.80	4,044
III	3,358–1,992	16.39–17.60	17.05	2,560
IV	1,992–904	17.60–19.43	29.65	1,441
V	904–503	19.43–20.67	10.51	568
VI	503–180	20.67–23.17	16.12	452



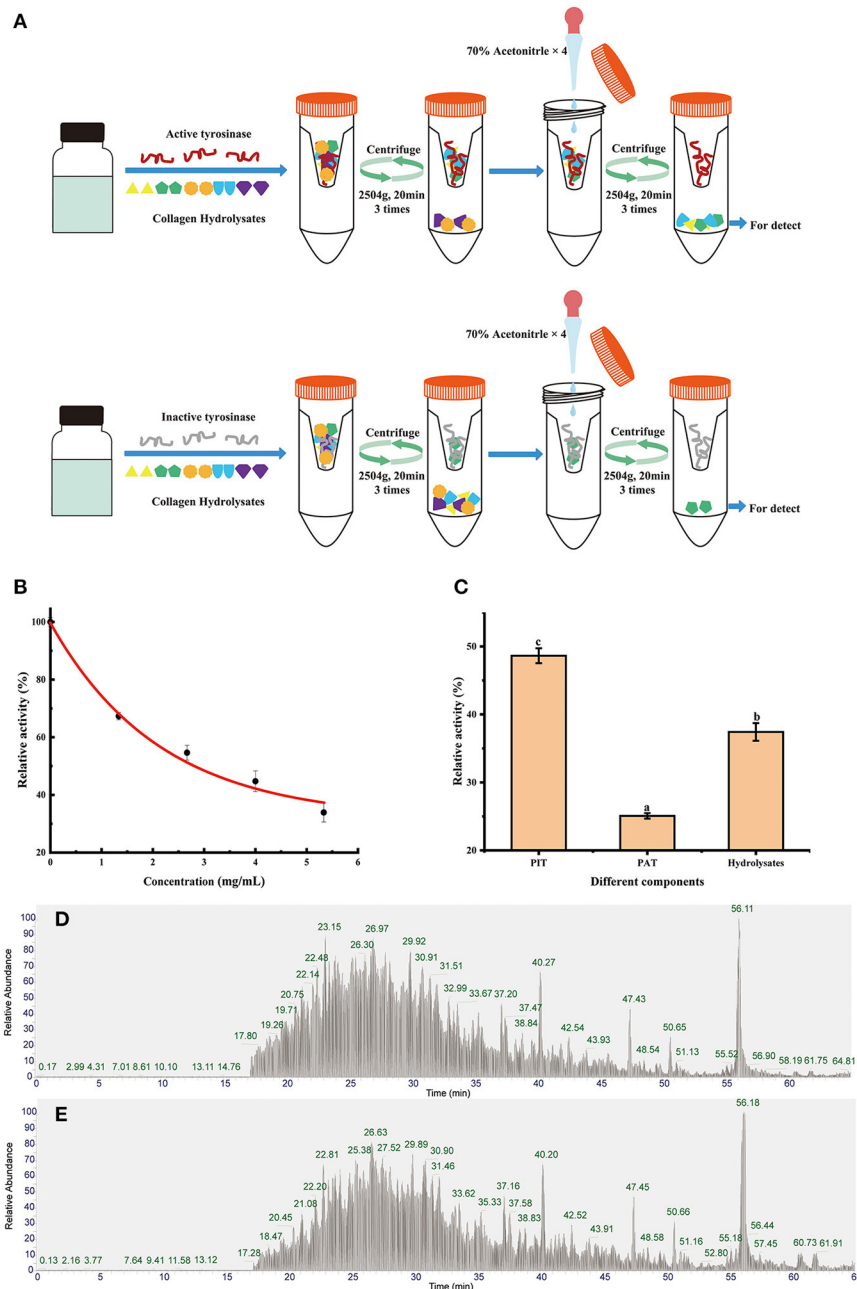


FIGURE 2 | Diagrams of biological affinity ultrafiltration—liquid mass spectrometry screening methods (A), the tyrosinase activity of hydrolysates (B), ultrafiltration fractions (C), the total ion chromatography (TIC) of PAT (D), and PIT (E). Different lowercase letters represent significant differences between different groups ($p < 0.05$).

where, A_s is the absorbance of experimental wells; A_c is the absorbance of control well; A_b is the absorbance of blank wells.

Statistical Analysis

In each analysis, three parallel tests were performed. The results were presented in the form of mean \pm standard deviation (SD). SPSS Statistics 20 software (IBM, Armonk, NY, USA) was used to perform one-way analysis of variance (ANOVA, $P < 0.05$) and Duncan's multiple range test to analyze the differences between samples.

RESULTS AND DISCUSSION

Amino Acid Composition and Molecular Weight Distribution of Hydrolysates

The amino acid composition of hydrolysates was shown in Table 1 and the total amount of amino acids was 67.12 g in 100 g hydrolysates. Many amino acid residues in collagen peptides are associated to tyrosinase inhibitory activity, according to the structure-activity relationship investigation between the peptide chain and melanin production inhibition (10, 33, 34).

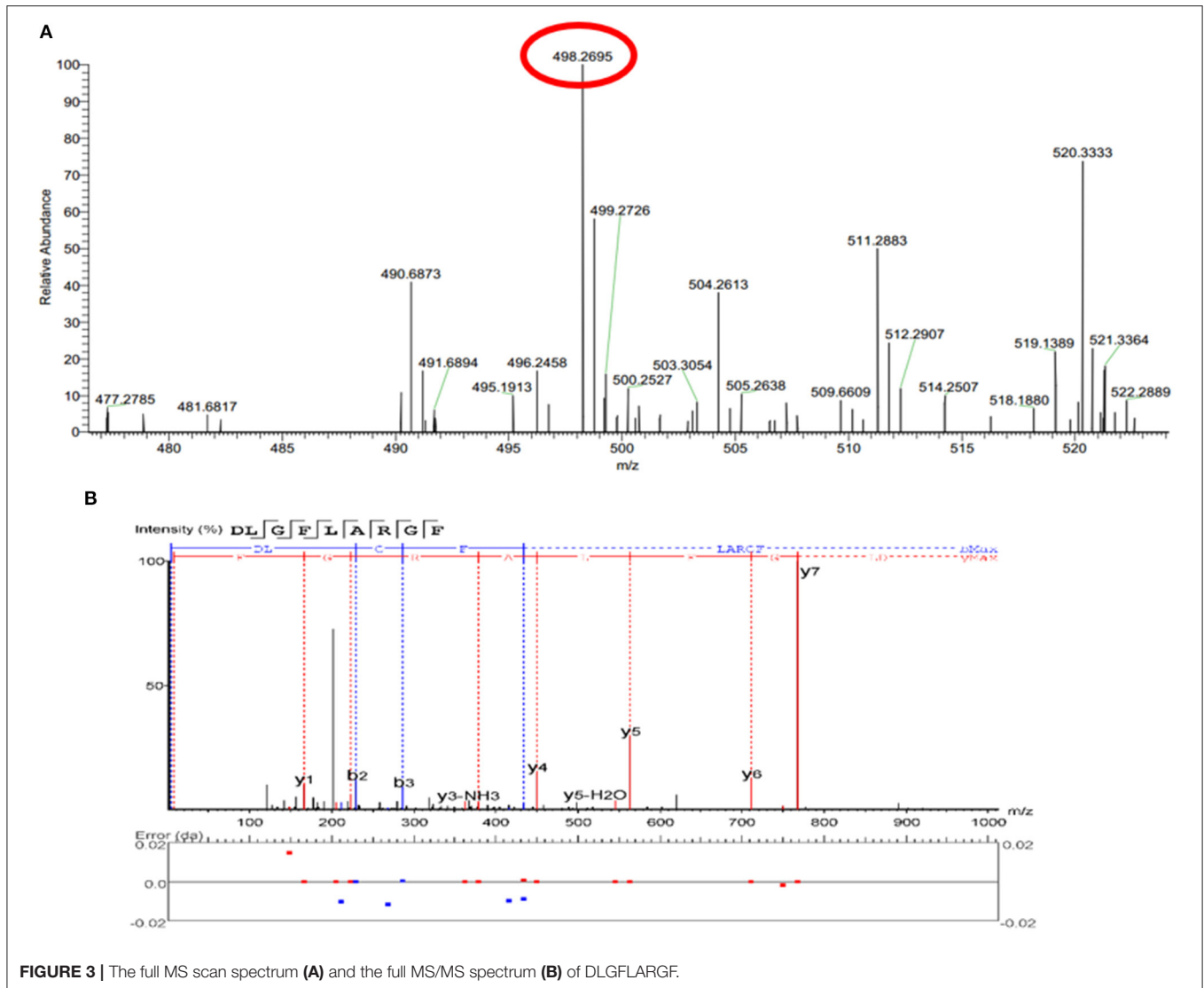


FIGURE 3 | The full MS scan spectrum (A) and the full MS/MS spectrum (B) of DLGFLARGF.

Val (V), Ala (A), Leu (L) and Ile (I) are four aliphatic hydrophobic amino acids that can directly interact with enzymes to inhibit the formation of dopaquinone, hence inhibiting melanin production, and have an additive effect. As shown in **Table 1**, the total amount of these four amino acids was 11.04 g/100 g hydrolysates, accounting for 16.45% of the total amino acid content. Arg (R) residues enhance cell penetration and facilitate the interaction between peptides and tyrosinase; Phe (F) is similar in structure to Tyr (Y) (the natural substrate of tyrosinase), which facilitates the binding of peptides and enzymes (10). The contents of these two amino acids were 6.74 g/100 g and 1.53 g/100 g in hydrolysates, respectively. Cys (C), Ser (S) and Thr (T) can form a complex with the enzymatic reaction product (dopaquinone) to prevent the conversion of dopaquinone into melanin, instead of inhibiting enzyme activity. The total amount of these three amino acids was 4.54 g/100 g in hydrolysates. Asp (D) and Glu (E) are negatively charged amino acid residues, which are not conducive to binding to tyrosinase. The total amount of these two amino acids was 12.40

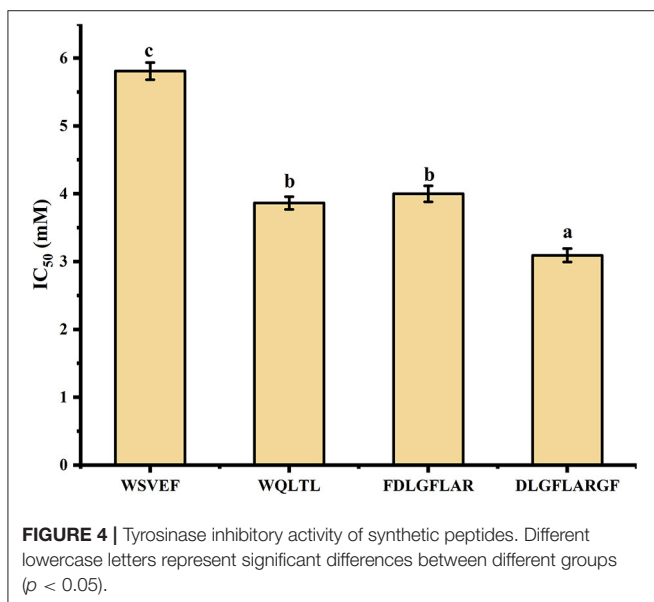
g/100 g hydrolysates, accounting for 18.47% of the total amino acid. From what has been discussed above, the content of amino acids beneficial to inhibiting melanin was up to 35.44%. These results suggested that hydrolysates may have strong tyrosinase inhibitory activity.

The MW distribution reflects the hydrolysis degree of fish scale gelatin (35). Peptides with different MW have different tyrosinase inhibition abilities (36). As shown in **Figure 1** and **Table 2**, there were mainly six peaks (I–VI), indicating that the hydrolysate contained six components, and the MW distribution of components I, II, III, IV, V and VI were 9,217–4,642 Da, 4,642–3,358 Da, 3,358–1,992 Da, 1,992–904 Da, 904–503 Da and 503–180 Da, respectively. The MW of the hydrolysates were mainly concentrated in components III, IV, V and VI, whose relative contents were 17.05, 29.65, 10.51, and 16.12%, accounting for more than 73% of the total contents. In addition, the MW of hydrolysates was mainly concentrated below 1,992 Da, accounting for 56.28% of proteolytic products. Alcalase is a non-specific protease that can cleave many sites in a protein at

TABLE 3 | Identification of peptides unique to PAT by LC-ESI-Q-Orbitrap-MS/MS.

No.	Peptide	RT (min)	Length	ALC (%)	m/z	Mass	Local confidence (%)
1	PGPVGVKL	27.98	8	99	383.7446	765.4749	99 100 100 100 100 100 100 100
2	LDALNENK	20.2	8	99	458.7404	915.4661	100 100 100 99 98 99 98 100
3	VPGPM	25.62	5	98	500.2538	499.2465	99 99 100 99 98
4	GPVGSF	29.02	6	98	563.2829	562.2751	97 98 99 99 100 100
5	TGPLGL	34.4	6	98	557.3301	556.322	97 98 99 99 100
6	FDLGFLAR*	42.62	8	98	469.7591	937.5021	99 99 99 98 98 97 97 99
7	FSGM	24.61	4	97	441.1804	440.1729	96 96 100 99
8	WSVEF*	45.45	5	97	667.3090	666.3013	93 95 100 100 100
9	GEPGLLGM	42.87	8	97	773.3893	772.3789	89 95 97 98 99 100 99 100
10	GPPGLLQQR	20.59	8	96	391.2201	780.4242	99 99 100 98 97 94 90 95
11	WQLTL*	47.88	5	96	660.3729	659.3643	97 94 99 96 95
12	EAPDPF	50.31	6	95	675.3026	674.2911	96 94 97 98 92 96
13	LVGPAQTQR	21.96	10	95	498.2855	994.5560	100 100 100 100 99 99 91 86 85 93
14	DAPGLLRGF	35.7	9	95	473.2618	944.5079	79 88 100 100 100 99 97 95 99
15	DLGFLARGF*	45.92	9	95	498.2695	994.5236	81 82 99 100 100 99 98 99 99
16	GFTGM	28.03	5	95	512.2175	511.2101	90 92 98 99 97

The above refers to the molecular mass less than or equal to 1,000 Da. The proportion of amino acids that are marked with * means that the contribution of tyrosinase inhibition is greater than or equal to 0.6.



random and generate a higher number of low MW peptides (37), which are attractive for higher biofunctional activity (38).

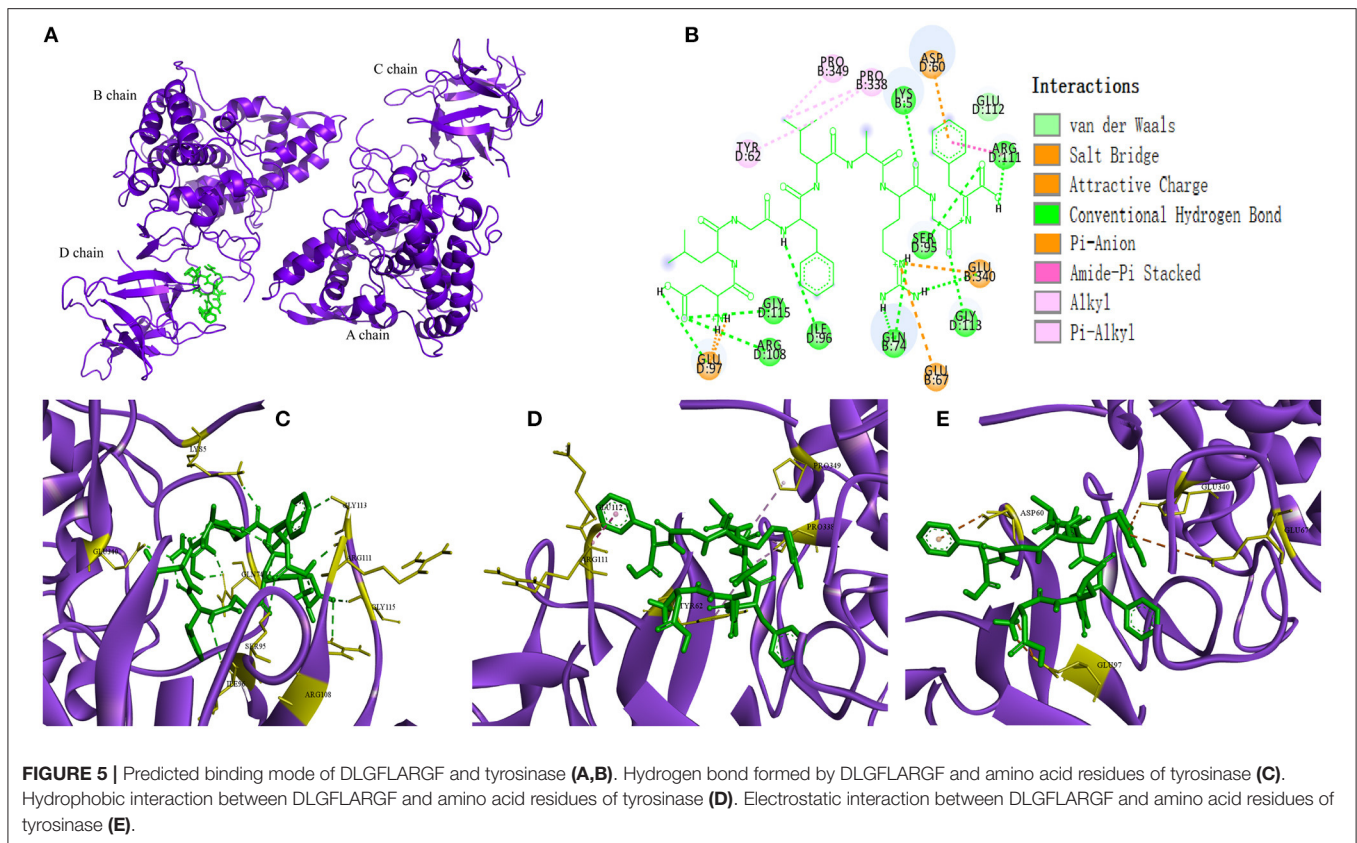
Enrichment and Identification of Potential TYIPs

Appropriate concentration and ratio are required in order to achieve a saturated state of binding. **Figure 2B** shows the tyrosinase activity residual rate of hydrolysates with different concentrations. Significant dose-dependence was observed in the concentration range of 0–5.33 mg/ml, which indicated that most of the active sites of tyrosinase can be bound by peptides. However, the inhibitory effect per milligram

of inhibitor decreased as the hydrolysates concentration increased. In order to retain an ideal tyrosinase inhibitory activity, the concentration of hydrolysates was set at 5 mg/ml with tyrosinase inhibitory activity rate at 61.7% for screening.

After bioaffinity ultrafiltration, tyrosinase inhibitions of PAT and PIT were evaluated. The results are shown in **Figure 2C**. The inhibition rate of tyrosinase on PAT was 74.92%, while the corresponding inhibition rates of PIT and hydrolysates were 51.37 and 62.58%, respectively. This suggests that certain peptides in the hydrolysates can specifically bind to the active site of tyrosinase and can be enriched effectively by bioaffinity ultrafiltration, resulting in a higher inhibition of PAT than PIT and hydrolysates.

The peptide composition in PAT and PIT was identified by Nano-LC-Q-Orbitrap-MS/MS to screen potential TYIPs. The total ion chromatograms were shown in **Figures 2D,E**. By matching the b and y series ions detected in the MS/MS spectrum with that recorded in database (uniprot-taxonomy Anabantaria 201912), the exact amino acid sequence of each peptide can be drawn. For example, peptide 9 (**Figure 3A**) has MS ion 498.2695^{2+} , b series of b2 (229.1183^{2+}), b3 (286.1397^{2+}) and b4 (433.2082^{2+}), y1 (166.0863^{2+}), y2 (223.1077^{2+}), y3 (379.2088^{2+}), y4 (450.2459^{2+}), y5 (563.3300^{2+}), y6 (710.3984^{2+}) and y7 (767.4199^{2+}), and the sequence was identified as DLGFLARGF (**Figure 3B**). By this method, 52 of the peptides identified in PAT were not found in PIT. Inhibitors can bind specifically to the active site of tyrosinase and be released by acetonitrile (39), which confirmed the high selectivity of bioaffinity ultrafiltration. Therefore, these specific peptides in PAT are considered as potential TYIPs.



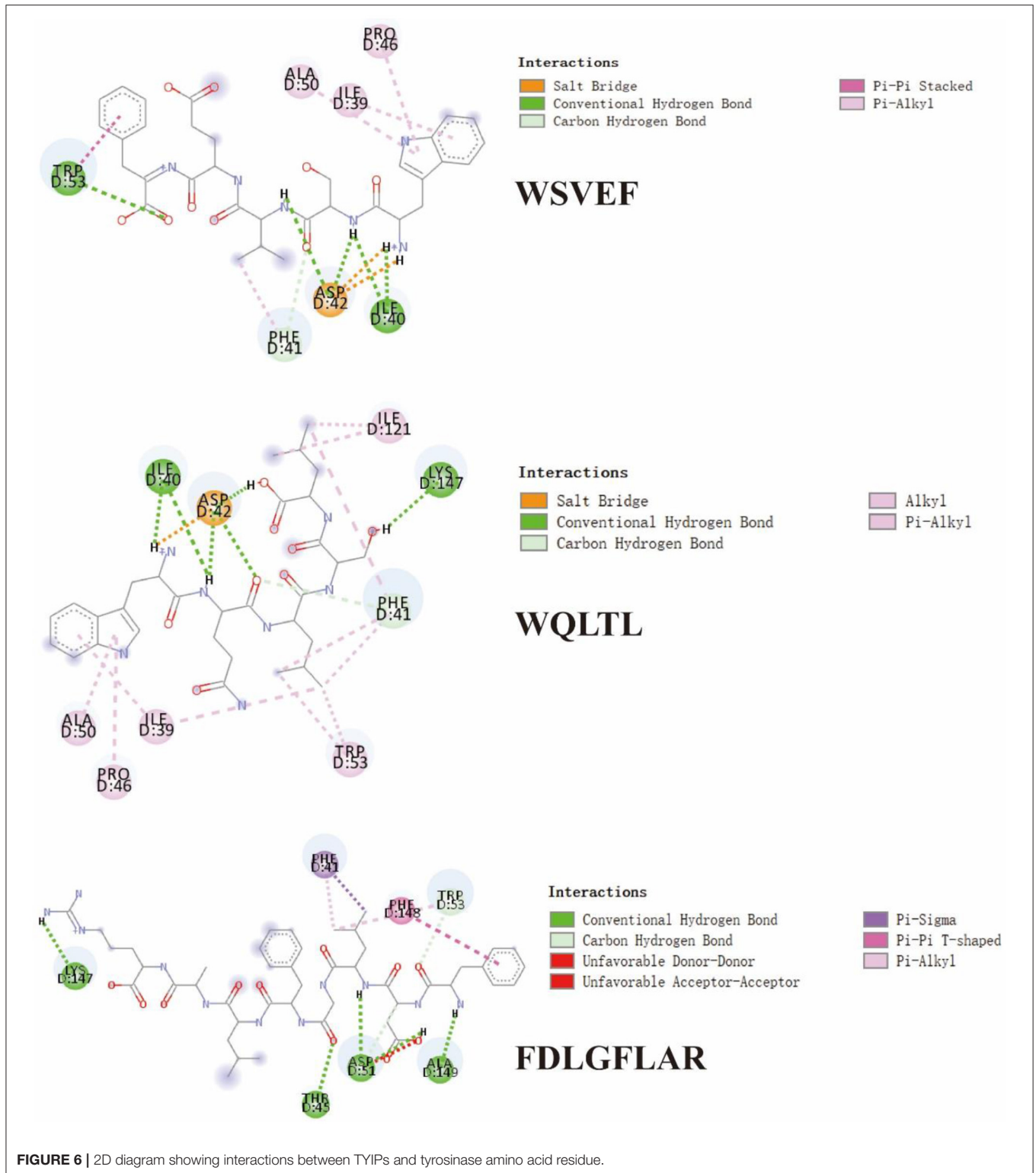
Rapid Screening and Tyrosinase Inhibitory Activity Verification

Studies have shown that peptides with lower MW tend to have higher functional activity (38). Therefore, peptides with MW $\leq 1,000$ Da were selected from the 52 peptides obtained, and 16 peptides (shown in **Table 3**) were obtained for subsequent analysis. Section Amino Acid Composition and Molecular Weight Distribution of Hydrolysates introduced some amino acids that contribute to tyrosinase inhibition, such as Val, Ala, Leu, Ile, Arg, Phe, Cys, Ser, and Thr. According to the screening method from previous study (10), 16 peptides in **Table 3** were counted for their tyrosinase inhibitory contribution ratio of amino acids, and 4 peptides (marked * in **Table 3**) with a contribution ratio of amino acids greater than or equal to 0.6 were obtained, they were discovered to be novel peptides by searching the data on the website <http://www.uwm.edu.pl/biochemia/index.php/en/biopep>. Therefore, the four peptides were used for subsequent synthesis to verify the tyrosinase inhibitory activity *in vitro*, the purity of the synthetic peptides was more than 95%. The tyrosinase inhibition ability of the synthetic peptide was shown in **Figure 4**. The peptide DLGFLARGF showed the strongest tyrosinase inhibition ability, with an IC_{50} value of 3.09 mM. The IC_{50} of peptides WQLTL, WSEVF and FDLGFLAR were 3.86, 5.81, and 4.00 mM, respectively, and they all showed good tyrosinase inhibitory activity. Similar peptides from natural sources have also been found in other studies, such as Phe-Pro-Tyr (FPY) from defatted walnut (*Juglans*

regia L.) meal hydrolysate with an IC_{50} value of 3.22 ± 0.22 mM (40), and RHAKF from Chinese quince seed protein hydrolysate with IC_{50} value of 1.15 mg/ml (41). In order to further explore the reasons for the difference in tyrosinase inhibition of these four peptides, molecular docking analysis was performed.

Molecular Docking

In recent years, as a computer simulation technology, molecular docking has been widely used to study the possible interaction mechanism between inhibitors and enzymes (42–44). In order to show the binding mode of TYIPs with tyrosinase more intuitively, the AutoDock tool was used, and the results are shown in **Figures 5, 6**. Peptide DLGFLARGF bonded to the D chain of tyrosinase and interacted with its surrounding amino acid residues, nine hydrogen bonds were formed with Glu 340, Arg 111, Gly 115, Arg 108, Ile 96, Ser 95, Gly 113, Lys 5 and Glu 97 on the enzyme D chain (**Figure 5C**). In addition, amino acid residues Try 62, Pro 338, Pro 349, Glu 112, and Arg 111 can form a hydrophobic pocket on the enzyme D chain, which tightly surround and hold the peptide DLGFLARGF through hydrophobic action (**Figure 5D**). At the same time, electrostatic interaction also occurred between Glu 97, Glu 340, Glu 67, Asp 60 and the peptide DLGFLARGF on the D-chain (as shown in **Figure 5E**). These results intuitively indicated that hydrogen bonding was the main driving force (as shown in **Table 4**) involved in the interaction between



peptide DLGFLARGF and tyrosinase. It can be inferred that the peptide DLGFLARGF binds to the inactive center of tyrosinase through hydrogen bonding, and indirectly inhibits the

binding of substrate to tyrosinase by changing the conformation of the enzyme, thereby inhibiting the catalytic activity of the enzyme.

TABLE 4 | Docking results according to hydrophobic interaction, electrostatic interaction and hydrogen bond for complex.

	DLGFLARGF	WQLTL	WSEVF	FDLGFLAR
Hydrogen bonds	Glu 340, Arg 111, Gly 115, Arg 108, Ile 96, Ser 95, Gly 113, Lys 5, Glu 97	Asp 42, Lys 147, Ile 40	Asp 42, Ile 40, Trp 53	Ala 149, Asp 51, Thr 45, Lys 147
Electrostatic interaction	Glu 97, Glu 340, Glu 67, Asp 60	Asp 42	Asp 42	No
Hydrophobic interaction	Tyr 62, Pro 338, Pro 349	Ile 121, Ile 39, Pro 46, Ala 50, Trp 53, Phe 41	Trp 53, Phe 41, Pro 46, Ala 50, Ile 39	Phe 148, Trp 53, Phe 41

In **Figure 6** and **Table 4**, it could be seen that driving forces in the peptides WQLTL, WSEVF, and FDLGFLAR were less than DLGFLARGF, which also led to lower tyrosinase inhibitory activity of these peptides. Moreover, molecular docking can also be used to screen enzyme inhibitors based on binding energy changes (45, 46). The three peptides have different binding energies with WQLTL = -8.3 kcal/mol, WSEVF = -9.2 kcal/mol, FDLGFLAR = -6.4 kcal/mol, which was not completely consistent with the trend of tyrosinase inhibition ability in **Figure 4**. This may be because the most stable conformation was selected based on the lowest binding energy, but the peptide conformation in the reaction system may not be the most stable (47). On the other hand, it may also be due to the longer-chain of FDLGFLAR closer to the center of the hydrophobic cavity and the more hydrophobic interactions of WQLTL than WSEVF.

The Effect of DLGFLARGF on B16F10 Melanoma Cells

The CCK-8 method was used to determine the potential cytotoxicity of different concentrations of DLGFLARGF compared with kojic acid (0.75 mg/ml). **Figure 7A** shows the effect of DLGFLARGF and kojic acid on the viability of B16F10 cells. With the increase of DLGFLARGF concentration, the cell survival rate gradually decreased. But within the tested concentration range (0–1.6 mg/ml), no obvious cytotoxicity was obtained (viability > 50%). Therefore, the concentrations of 0, 0.1, 0.2, 0.4, 0.8, and 1.6 mg/ml were selected to study the inhibitory effect of DLGFLARGF on melanin synthesis.

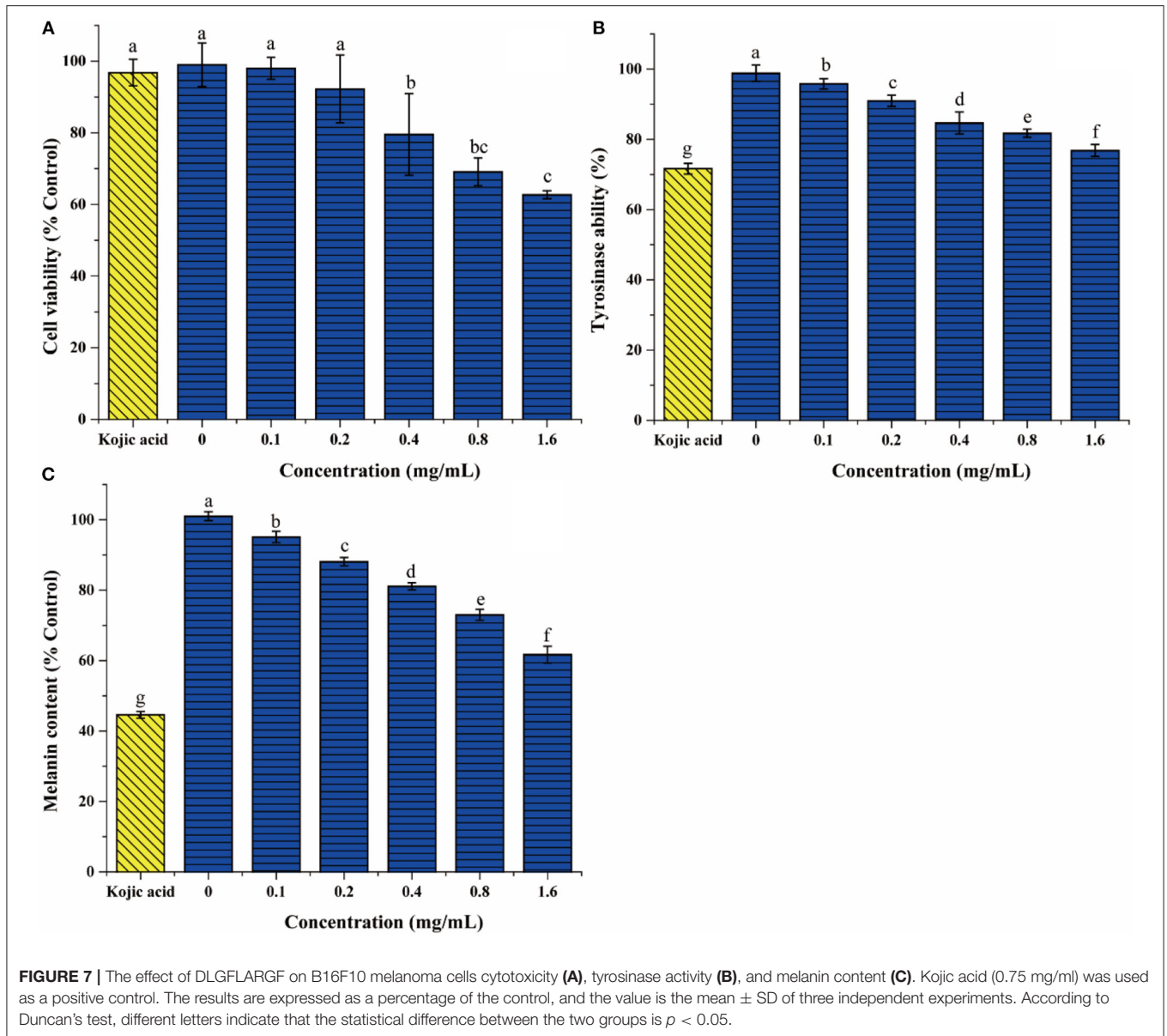
To further evaluate the tyrosinase inhibition of DLGFLARGF, B16F10 melanoma cells were treated with different concentrations of DLGFLARGF and kojic acid (0.75 mg/ml). The result is shown in **Figure 7B**. With the increase of DLGFLARGF concentration, tyrosinase activity gradually decreased, indicating gradually increased tyrosinase inhibitory ability. The inhibition rate was 23.19% for 1.6 mg/ml of DLGFLARGF, which was very

close to that of kojic acid with 28.34% inhibition rate under 0.75 mg/ml. According to the previous results, the peptide DLGFLARGF was found to reduce tyrosinase activity by binding to the amino acid residue sites on the D chain of tyrosinase upon entry into the cells, but kojic acid in published study was proved to be docked to the catalytic site of mushroom tyrosinase and thus had a stronger tyrosinase inhibitory activity (48).

The content of melanin can directly determines the degree of skin whiteness. At present, the recognized process of melanin formation is roughly that tyrosine is oxidized to dopa under the action of tyrosinase, and then dopa is oxidized to dopa-quinone, which finally forms eumelanin through a series of reactions. Tyrosinase is the key enzyme for melanin formation (49). As shown in **Figure 7C**, the melanin content gradually decreased as the concentration of DLGFLARGF increased and showed a concentration-dependent relationship, indicating that DLGFLARGF can effectively inhibit the production of melanin. In terms of the inhibitory effects on melanin production, the melanin content was reduced by 55.4% in the cells treated with kojic acid (0.75 mg/ml), while DLGFLARGF reduced by 38.3% at 1.6 mg/ml. Kojic acid had been proved to be better than DLGFLARGF in inhibiting tyrosinase activity. On the other hand, the synthesis of melanin involves various factors besides tyrosinase, and kojic acid could also regulate transcription of tyrosinase pathway genes and bleach produced melanin (50). Moreover, collagen peptide has mild functional activity, easy absorption and high skin compatibility, while kojic acid lacks good permeability in application, and show high toxicity and low activity stability (51).

CONCLUSIONS

In this work, the alcalase hydrolysate of grass carp fish scale gelatin was discovered to have promising tyrosinase inhibitory activity. The tyrosinase inhibition rate of fish scale gelatin treated with alcalase was 61.7% (at 5 mg/ml). The MW distribution of the hydrolysate was mainly below 3,358 Da (73.33%), and the content of amino acids that inhibit melanin was up to 35.44%. A rapid screening method of TYIPs based on bioaffinity ultrafiltration combined with LC-Orbitrap-MS/MS was established. 52 peptides were identified from PAT, among which 4 new peptides were screened. The peptide DLGFLARGF showed excellent tyrosinase inhibitory activity with an IC_{50} value of 3.09 mM. Hydrogen bonds were the predominant driving force in the interaction between peptide DLGFLARGF and tyrosinase according to molecular docking. In addition, when the concentration of DLGFLARGF reached 1.6 mg/ml, the melanin content and tyrosinase activity decreased to 61.7% and 76.81% of the control group, respectively. The above results indicate that bioaffinity ultrafiltration combined with LC-Orbitrap-MS/MS is an effective method for high-throughput screening of TYIPs. Moreover, DLGFLARGF can be widely used as a tyrosinase inhibitor in the whitening foods and pharmaceuticals.



DATA AVAILABILITY STATEMENT

The original contributions presented in the study are included in the article/supplementary material, further inquiries can be directed to the corresponding authors.

AUTHOR CONTRIBUTIONS

Z-ZH: experiments, data curation, and writing-original draft. X-MS: supervision, review, and editing. LZ: investigation,

methodology, review, and editing. M-JZ: experiments. Z-CT: project administration, supervision, and funding acquisition. All authors contributed to the article and approved the submitted version.

FUNDING

This study was supported by the National Key R&D Program of China (No. 2018YFD0901101).

REFERENCES

- Sha XM, Hu ZZ, Tu ZC, Zhang LZ, Duan DL, Huang T, et al. Influence of dynamic high pressure microfluidization on functional properties and structure of gelatin from bighead carp (*Hypophthalmichthys nobilis*) scale. *J Food Process Preserv.* (2018) 42:e13607. doi: 10.1111/jfpp.13607
- Sow LC, Nicholas ZYT, Wong CW, Yang H. Combination of sodium alginate with tilapia fish gelatin for improved texture

- properties and nanostructure modification. *Food Hydrocoll.* (2019) 94:459–67. doi: 10.1016/j.foodhyd.2019.03.041
3. Sow LC, Tana SJ, Yang H. Rheological properties and structure modification in liquid and gel of tilapia skin gelatin by the addition of low acyl gellan. *Food Hydrocoll.* (2019) 90:9–18. doi: 10.1016/j.foodhyd.2018.12.006
 4. Zhao X, Zhou Y, Zhao L, Chen L, He Y, Yang H. Vacuum impregnation of fish gelatin combined with grape seed extract inhibits protein oxidation and degradation of chilled tilapia fillets. *Food Chem.* (2019) 294:316–25. doi: 10.1016/j.foodchem.2019.05.054
 5. Xin Y, Chai M, Chen F, Hou Y, Lai S, Yang H. Comparative study on the gel properties and nanostructures of gelatins from chicken, porcine, and tilapia skin. *J Food Sci.* (2021) 86:1936–45. doi: 10.1111/1750-3841.15700
 6. Zhang YF, Duan X, Zhuang YL. Purification and characterization of novel antioxidant peptides from enzymatic hydrolysates of tilapia (*Oreochromis niloticus*) skin gelatin. *Peptides.* (2012) 38:13–21. doi: 10.1016/j.peptides.2012.08.014
 7. Lin L, Lv S, Li BF. Angiotensin-I-converting enzyme (ACE)-inhibitory and antihypertensive properties of squid skin gelatin hydrolysates. *Food Chem.* (2012) 131:225–30. doi: 10.1016/j.foodchem.2011.08.064
 8. Wang FH, Dong XF, Xiu P, Zhong JT, Wei HL, Xu ZZ, et al. T7 peptide inhibits angiogenesis via downregulation of angiopoietin-2 and autophagy. *Oncol Rep.* (2015) 33:675–84. doi: 10.3892/or.2014.3653
 9. Ennaas N, Hammami R, Beaulieu L, Fliss I. Purification and characterization of four antibacterial peptides from protamex hydrolysate of Atlantic mackerel (*Scomber scombrus*) by-products. *Biochem Biophys Res Commun.* (2015) 462:195–200. doi: 10.1016/j.bbrc.2015.04.091
 10. Schurink M, van Berkel WJH, Wichers HJ, Boeriu CG. Novel peptides with tyrosinase inhibitory activity. *Peptides.* (2007) 28:485–95. doi: 10.1016/j.peptides.2006.11.023
 11. Wu JJ, Lin JC, Wang CH, Jong TT, Yang HL, Hsu SL, et al. Extraction of antioxidative compounds from wine lees using supercritical fluids and associated anti-tyrosinase activity. *J Supercrit Fluids.* (2009) 50:33–41. doi: 10.1016/j.supflu.2009.04.010
 12. Kameyama K, Sakai C, Kuge S, Nishiyama S, Tomita Y, Ito S, et al. The expression of tyrosinase, tyrosinase-related proteins 1 and 2 (TRP1 and TRP2), the silver protein, and a melanogenic inhibitor in human melanoma cells of differing melanogenic activities. *Pigm Cell Res.* (1995) 8:97–104. doi: 10.1111/j.1600-0749.1995.tb00648.x
 13. Patil S, Sistla S, Jadhav J. Screening of inhibitors for mushroom tyrosinase using surface plasmon resonance. *J Agric Food Chem.* (2014) 62:11594–601. doi: 10.1021/jf5039585
 14. Lee SY, Baek N, and Nam T-g. Natural, semisynthetic and synthetic tyrosinase inhibitors. *J Enzyme Inhib Med Chem.* (2016) 31:1–13. doi: 10.3109/14756366.2015.1004058
 15. Song X, Hu X, Zhang Y, Pan J, Gong D, Zhang G. Inhibitory mechanism of epicatechin gallate on tyrosinase: inhibitory interaction, conformational change and computational simulation. *Food Funct.* (2020) 11:4892–902. doi: 10.1039/D0FO00003E
 16. Hemachandran H, Jain F, Mohan S, Kumar DT, Priya Doss CG, Ramamoorthy S. Glandular hair constituents of *Mallotus philippinensis* Muell. fruit act as tyrosinase inhibitors: Insights from enzyme kinetics and simulation study. *Int J Biol Macromol.* (2018) 107:1675–82. doi: 10.1016/j.ijbiomac.2017.10.036
 17. Anantharaman A, Hemachandran H, Mohan S, Ayyathan DM, Kumar DT, Doss CGP, et al. Induction of apoptosis by apocarotenoids in B16 melanoma cells through ROS-mediated mitochondrial-dependent pathway. *J Funct Foods.* (2016) 20:346–57. doi: 10.1016/j.jff.2015.11.019
 18. Hridya H, Amrita A, Mohan S, Gopalakrishnan M, Dakshinamurthy TK, Doss GP, et al. Functionality study of santalin as tyrosinase inhibitor: a potential depigmentation agent. *Int J Biol Macromol.* (2016) 86:383–9. doi: 10.1016/j.ijbiomac.2016.01.098
 19. Thaha A, Wang BS, Chang YW, Hsia SM, Huang TC, Shiau CY, et al. Food-derived bioactive peptides with antioxidative capacity, xanthine oxidase and tyrosinase inhibitory activity. *Processes.* (2021) 9:747. doi: 10.3390/pr9050747
 20. Wu QY, Jia JQ, Yan H, Du JJ, Gui ZZ. A novel angiotensin-I converting enzyme (ACE) inhibitory peptide from gastrointestinal protease hydrolysate of silkworm pupa (*Bombyx mori*) protein: biochemical characterization and molecular docking study. *Peptides.* (2015) 68:17–24. doi: 10.1016/j.peptides.2014.07.026
 21. Zhong C, Sun LC, Yan LJ, Lin YC, Liu GM, Cao MJ. Production, optimisation and characterisation of angiotensin converting enzyme inhibitory peptides from sea cucumber (*Stichopus japonicus*) gonad. *Food Funct.* (2018) 9:594–603. doi: 10.1039/c7fo01388d
 22. Wang L, Liu YF, Luo Y, Huang KY, Wu ZQ. Quickly screening for potential alpha-glucosidase inhibitors from guava leaves tea by bioaffinity ultrafiltration coupled with HPLC-ESI-TOF/MS method. *J Agric Food Chem.* (2018) 66:1576–82. doi: 10.1021/acs.jafc.7b05280
 23. Zhang L, Xu L, Ye YH, Zhu MF, Li J, Tu ZC, et al. Phytochemical profiles and screening of alpha-glucosidase inhibitors of four Acer species leaves with ultra-filtration combined with UPLC-QTOF-MS/MS. *Ind Crop Prod.* (2019) 129:156–68. doi: 10.1016/j.indcrop.2018.11.051
 24. Qin SS, Ren YR, Fu X, Shen J, Chen X, Wang Q, et al. Multiple ligand detection and affinity measurement by ultrafiltration and mass spectrometry analysis applied to fragment mixture screening. *Anal Chim Acta.* (2015) 886:98–106. doi: 10.1016/j.aca.2015.06.017
 25. Sha XM, Tu ZC, Liu W, Wang H, Shi Y, Huang T, et al. Effect of ammonium sulfate fractional precipitation on gel strength and characteristics of gelatin from bighead carp (*Hypophthalmichthys nobilis*) scale. *Food Hydrocoll.* (2014) 36:173–80. doi: 10.1016/j.foodhyd.2013.09.024
 26. Uysal S, Zengin G, Locatelli M, Bahadori MB, Mocan A, Bellagamba G, et al. Cytotoxic and enzyme inhibitory potential of two potentilla species (*P-speciosa* L. and *P-reptans* Willd) and their chemical composition. *Front Pharmacol.* (2017) 8:290. doi: 10.3389/fphar.2017.00290
 27. Chen X, Wu JH, Li L, Wang SY. Cryoprotective activity and action mechanism of antifreeze peptides obtained from tilapia scales on *Streptococcus thermophilus* during cold stress. *J Agric Food Chem.* (2019) 67:1918–26. doi: 10.1021/acs.jafc.8b06514
 28. Jiang X, Cui ZQ, Wang LH, Xu HJ, Zhang YG. Production of bioactive peptides from corn gluten meal by solid-state fermentation with *Bacillus subtilis* MTCC5480 and evaluation of its antioxidant capacity *in vivo*. *LWT-Food Sci Technol.* (2020) 131:109767. doi: 10.1016/j.lwt.2020.109767
 29. Ismaya WT, Rozeboom HJ, Weijn A, Mes JJ, Fusetti F, Wichers HJ, et al. Crystal Structure of Agaricus bisporus Mushroom Tyrosinase: Identity of the Tetramer Subunits and Interaction with Tropolone. *Biochemistry.* (2011) 50:5477–86. doi: 10.1021/bi200395t
 30. Munetaka I, Hideyuki T, Masanobu S, Kazumi S, Yosuke O, Keiyu U. A combined assay of cell viability and *in vitro* cytotoxicity with a highly water-soluble tetrazolium salt, neutral red and crystal violet. *Biol Pharm Bull.* (1996) 19:1518–20. doi: 10.1248/bpb.19.1518
 31. Ullah S, Park Y, Park C, Lee S, Kang D, Yang J, et al. Antioxidant, anti-tyrosinase and anti-melanogenic effects of (E)-2,3-diphenylacrylic acid derivatives. *Bioorg Med Chem.* (2019) 27:2192–200. doi: 10.1016/j.bmc.2019.04.020
 32. Zhang X, Li J, Li Y, Liu Z, Lin Y, Huang J. Anti-melanogenic effects of epigallocatechin-3-gallate (EGCG), epicatechin-3-gallate (ECG) and gallicocatechin-3-gallate (GCG) via down-regulation of cAMP/CREB/MITF signaling pathway in B16F10 melanoma cells. *Fitoterapia.* (2020) 145:104634. doi: 10.1016/j.fitote.2020.104634
 33. Futaki S. Membrane-permeable arginine-rich peptides and the translocation mechanisms. *Adv Drug Delivery Rev.* (2005) 57:547–58. doi: 10.1016/j.addr.2004.10.009
 34. Ishikawa M, Kawase I, Ishii F. Combination of amino acids reduces pigmentation in B16F0 melanoma cells. *Biol Pharm Bull.* (2007) 30:677–81. doi: 10.1248/Bpb.30.677
 35. Chen SY, Yang Q, Chen X, Tian YQ, Liu ZY, Wang SY. Bioactive peptides derived from crimson snapper and *in vivo* anti-aging effects on fat diet-induced high fat *Drosophila melanogaster*. *Food Funct.* (2020) 11:524–33. doi: 10.1039/c9fo01414d
 36. Zhuang YL, Sun LP, Zhao X, Wang JF, Hou H, Li BF. Antioxidant and melanogenesis-inhibitory activities of collagen peptide from jellyfish (*Rhopilema esculentum*). *J Sci Food Agric.* (2009) 89:1722–7. doi: 10.1002/jsfa.3645
 37. Maqsoodlou A, Mahoonak AS, Mora L, Mohebodini H, Toldrá F, Ghorbani M. Peptide identification in alcalase hydrolysed pollen and comparison of its bioactivity with royal jelly. *Food Res Int.* (2019) 116:905–15. doi: 10.1016/j.foodres.2018.09.027

38. Chen N, Yang HM, Sun Y, Niu J, Liu S. Purification and identification of antioxidant peptides from walnut (*Juglans regia* L) protein hydrolysates. *Peptides*. (2012) 38:344–9. doi: 10.1016/j.peptides.2012.09.017
39. Mulabagal V, Calderon AI. Development of an ultrafiltration-liquid chromatography/mass spectrometry (UF-LC/MS) based ligand-binding assay and an LC/MS based functional assay for mycobacterium tuberculosis shikimate kinase. *Anal Chem*. (2010) 82:3616–21. doi: 10.1021/ac902849g
40. Feng YX, Wang ZC, Chen JX, Li HR, Wang YB, Ren DF, et al. Separation, identification, and molecular docking of tyrosinase inhibitory peptides from the hydrolysates of defatted walnut (*Juglans regia* L). meal. *Food Chem*. (2021) 353:129471. doi: 10.1016/j.foodchem.2021.129471
41. Deng YJ, Huang LX, Zhang CH, Xie PJ, Cheng J, Wang X, et al. Skin-care functions of peptides prepared from Chinese quince seed protein: sequences analysis, tyrosinase inhibition and molecular docking study. *Ind Crop Prod*. (2020) 148:112331. doi: 10.1016/j.indcrop.2020.112331
42. Chai WM, Lin MZ, Song FJ, Wang YX, Xu KL, Huang JX, et al. Rifampicin as a novel tyrosinase inhibitor: Inhibitory activity and mechanism. *Int J Biol Macromol*. (2017) 102:425–30. doi: 10.1016/j.ijbiomac.2017.04.058
43. Hridya H, Amrita A, Sankari M, Doss CGP, Gopalakrishnan M, Gopalakrishnan C, et al. Inhibitory effect of brazilein on tyrosinase and melanin synthesis: kinetics and in silico approach. *Int J Biol Macromol*. (2015) 81:228–34. doi: 10.1016/j.ijbiomac.2015.07.064
44. Wang YJ, Zhang GW, Yan JK, Gong DM. Inhibitory effect of morin on tyrosinase: Insights from spectroscopic and molecular docking studies. *Food Chem*. (2014) 163:226–33. doi: 10.1016/j.foodchem.2014.04.106
45. Kharazmi Khorassani J, Asoodeh A, Tanzadehpanah H. Antioxidant and angiotensin-converting enzyme-ACE-inhibitory activity of thymosin alpha-1-Thα1-peptide. *Bioorg Chem*. (2019) 87:743–52. doi: 10.1016/j.bioorg.2019.04.003
46. Wu HX, Liu YL, Guo MR, Xie JL, Jiang XM. A virtual screening method for inhibitory peptides of angiotensin I-converting enzyme. *J Food Sci*. (2014) 79:C1635–42. doi: 10.1111/1750-3841.12559
47. Ma TX, Fu QQ, Mei QG, Tu ZC, Zhang L. Extraction optimization and screening of angiotensin-converting enzyme inhibitory peptides from *Channa striatus* through bioaffinity ultrafiltration coupled with LC-Orbitrap-MS/MS and molecular docking. *Food Chem*. (2021) 354:129589. doi: 10.1016/j.foodchem.2021.129589
48. Söhretoglu D, Sari S, Barut B, Özel A. Tyrosinase inhibition by some flavonoids: Inhibitory activity, mechanism by *in vitro* and *in silico* studies. *Bioorg Chem*. (2018) 81:168–74. doi: 10.1016/j.bioorg.2018.08.020
49. Halaban. R, Patton RS, Cheng E, Svedine S, Trombetta ES, Wahl ML, et al. Abnormal acidification of melanoma cells induces tyrosinase retention in the early secretory pathway. *J. Biol. Chem*. (2002) 277:14821–8. doi: 10.1074/jbc.M111497200
50. Meng W, Zhang C, Xiao D. The effect of different activated carbon and bleaching temperature on kojic acid bleaching. Berlin: Springer (2015). p. 325–33.
51. Nerya O, Musa R, Khatib S, Tamir S, Vaya J. Chalcones as potent tyrosinase inhibitors: the effect of hydroxyl positions and numbers. *Phytochemistry*. (2004) 65:1389–95. doi: 10.1016/j.phytochem.2004.04.016

Conflict of Interest: The authors declare that the research was conducted in the absence of any commercial or financial relationships that could be construed as a potential conflict of interest.

The reviewer LZ declared a shared affiliation with the author Z-CT to the handling editor at the time of review.

Publisher's Note: All claims expressed in this article are solely those of the authors and do not necessarily represent those of their affiliated organizations, or those of the publisher, the editors and the reviewers. Any product that may be evaluated in this article, or claim that may be made by its manufacturer, is not guaranteed or endorsed by the publisher.

Copyright © 2022 Hu, Sha, Zhang, Zha and Tu. This is an open-access article distributed under the terms of the Creative Commons Attribution License (CC BY). The use, distribution or reproduction in other forums is permitted, provided the original author(s) and the copyright owner(s) are credited and that the original publication in this journal is cited, in accordance with accepted academic practice. No use, distribution or reproduction is permitted which does not comply with these terms.